

Kinetics of Acid-Catalyzed O-Atom Transfer from a Hydroperoxorhodium Complex to Organic and Inorganic Substrates

Kelemu Lemma and Andreja Bakac*

Ames Laboratory, Iowa State University of Science and Technology, Ames, Iowa 50011

Received May 4, 2004

Oxygen atom transfer from $(\text{NH}_3)_4(\text{H}_2\text{O})\text{RhOOH}^{2+}$ to organic and inorganic nucleophiles takes place according to the rate law $-\text{d}[(\text{NH}_3)_4(\text{H}_2\text{O})\text{RhOOH}^{2+}]/\text{dt} = k[\text{H}^+][(\text{NH}_3)_4(\text{H}_2\text{O})\text{RhOOH}^{2+}][\text{nucleophile}]$ for all the cases examined. The third-order rate constants were determined in aqueous solutions at 25 °C for $(\text{CH}_2)_5\text{S}$ ($k = 430 \text{ M}^{-2} \text{ s}^{-1}$, $\mu = 0.10 \text{ M}$), $(\text{CH}_2)_4\text{S}_2$ (182, $\mu = 0.10 \text{ M}$), $\text{CH}_3\text{CH}_2\text{SH}$ (8.0, $\mu = 0.20 \text{ M}$), $(\text{en})_2\text{Co}(\text{SCH}_2\text{CH}_2\text{NH}_2)^{2+}$ (711, $\mu = 0.20 \text{ M}$), and, in acetonitrile–water, CH_3SPh (130, 10% AN, $\mu = 0.20 \text{ M}$), PPh_3 (3.74×10^3 , 50% AN), and $(2\text{-C}_3\text{H}_7)_2\text{S}$ (45, 50% AN, $\mu = 0.20 \text{ M}$). Oxidation of PPh_3 by $(\text{NH}_3)_4(\text{H}_2\text{O})\text{Rh}^{18}\text{O}^{18}\text{OH}^{2+}$ produced $^{18}\text{OPPh}_3$. The reaction with a series of *p*-substituted triphenylphosphines yielded a linear Hammett relationship with $\rho = -0.53$. Nitrous acid ($k = 891 \text{ M}^{-2} \text{ s}^{-1}$) is less reactive than the more nucleophilic nitrite ion ($k = 1.54 \times 10^4 \text{ M}^{-2} \text{ s}^{-1}$).

Introduction

Typically, the 2-e (oxygen transfer) oxidation of nucleophilic substrates by hydrogen peroxide takes place in parallel acid-independent and acid-catalyzed pathways as shown in eq 1, where Nuc stands for nucleophile.^{1–3} On the other hand, metal hydroperoxides, LMOOH^{n+} , formally derived from H_2O_2 by replacing one of the hydrogen ions by a metal complex, react predominantly by acid-catalyzed routes, often without evidence for acid-independent pathways.^{4–7} We came across several examples of such chemistry in our recent work with hydroperoxorhodium cations of the general formula $\text{trans-L}(\text{H}_2\text{O})\text{RhOOH}^{2+}$ ($\text{L} = [14]\text{aneN}_4$ (L^1), *meso*- $\text{Me}_6[14]\text{-aneN}_4$ (L^2), and $(\text{NH}_3)_4$).⁴

$$\text{rate} = (k_o + k_H[\text{H}^+])[\text{H}_2\text{O}_2][\text{Nuc}] \quad (1)$$

The complex $(\text{NH}_3)_4(\text{H}_2\text{O})\text{RhOOH}^{2+}$ is the most reactive of the hydroperoxides we have investigated to date. In addition to its great reactivity, this material has several other

attractive properties for kinetic studies. Acidic aqueous solutions of $(\text{NH}_3)_4(\text{H}_2\text{O})\text{RhOOH}^{2+}$ are stable for days in a refrigerator. Also, there is a strong UV band at 241 nm ($\epsilon = 4000 \text{ M}^{-1} \text{ cm}^{-1}$), which facilitates kinetic measurements.

As part of our continued interest in oxygen atom transfer reactions, we have now carried out a kinetic and mechanistic study of the oxidation of a number of organic and inorganic substrates with $(\text{NH}_3)_4(\text{H}_2\text{O})\text{RhOOH}^{2+}$. In addition to establishing the previously observed features of oxygen atom transfer, we present further evidence for such a mechanism in the form of structure–reactivity relationships and isotopic labeling studies.

Experimental Section

A sample of $[(\text{NH}_3)_5\text{Rh}(\text{H})](\text{SO}_4)_4$ was available from our previous work. The complex $[(\text{en})_2\text{Co}(\text{SR})\text{Cl}_2 \cdot \text{H}_2\text{O}$ ($\text{R} = \text{CH}_2\text{CH}_2\text{NH}_2$) was prepared according to a literature method.⁸ Sodium nitrite (99.99+%), the sulfides, and most of the phosphines (Aldrich), (*p*- $\text{F-C}_6\text{H}_4$)₃P (Strem), perchloric acid, and sodium perchlorate (both Fisher) were reagent grade or better and used as received. Oxygen-18 ($^{18}\text{O}_2$, 95–98%) was supplied by Cambridge Isotope Laboratories.

Stock solutions of the sulfides, ethanethiol, and triarylphosphines were prepared in acetonitrile (AN), and those of $(\text{en})_2\text{Co}(\text{SCH}_2\text{CH}_2\text{NH}_2)^{2+}$ and NaNO_2 in water. Solutions of NaNO_2 were kept under argon in the dark. Concentrations of $(\text{en})_2\text{Co}(\text{SCH}_2\text{CH}_2\text{NH}_2)^{2+}$ were determined by spectrophotometric titration of dilute solutions with H_2O_2 in 0.10 M H^+ at 365 nm, where the product $(\text{en})_2\text{Co}(\text{S}(\text{O})\text{CH}_2\text{CH}_2\text{NH}_2)^{2+}$ has $\epsilon = 6700 \text{ M}^{-1} \text{ cm}^{-1}$.¹

(8) Nosco, D. L.; Deutsch, E. *Inorg. Synth.* **1982**, *21*, 19–23.

* To whom correspondence should be addressed. E-mail: bakac@ameslab.gov.

(1) Adzamlı, I. K.; Libson, K.; Lydon, J. D.; Elder, R. C.; Deutsch, E. *Inorg. Chem.* **1979**, *18*, 303–311.

(2) Mohammad, A.; Liebafsky, H. A. *J. Am. Chem. Soc.* **1934**, *56*, 1680–1685.

(3) Bakac, A.; Assink, B.; Espenson, J. H. *Inorg. Chem.* **1996**, *35*, 788–790.

(4) Lemma, K.; Bakac, A. *Inorg. Chem.* **2004**, *43*, 4505–4510.

(5) Mirza, S. A.; Bocquet, B.; Robyr, C.; Thomi, S.; Williams, A. F. *Inorg. Chem.* **1996**, *35*, 1332–1337.

(6) Bakac, A. *Prog. Inorg. Chem.* **1995**, *43*, 267–351.

(7) Bakac, A. *Adv. Inorg. Chem.* **2004**, *55*, 1–59.

Aqueous stock solutions of $(\text{NH}_3)_4(\text{H}_2\text{O})\text{RhOOH}^{2+}$ were prepared from the parent hydride and O_2 as previously described.⁹ The concentrations were determined from the absorbance at 241 nm ($\epsilon = 4000 \text{ M}^{-1} \text{ cm}^{-1}$).¹⁰ Deionized water was further purified by passage through a Millipore Q water purification system.

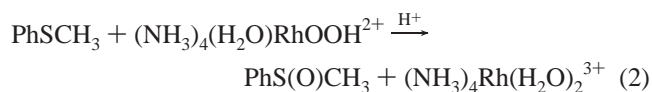
UV-vis spectra and kinetic measurements were performed with use of a conventional UV-vis Shimadzu 3101 PC spectrometer. After it was ascertained that the kinetics were unaffected by the presence of O_2 , no effort was made to keep the solutions air-free. Data analysis was performed by use of KaleidaGraph 3.09 PC software.

All the substrates were used in large excess (at least 10-fold) over $(\text{NH}_3)_4(\text{H}_2\text{O})\text{RhOOH}^{2+}$ to maintain pseudo-first-order conditions. Aliphatic sulfides do not absorb strongly in the UV, and their reactions were monitored by observing the loss of $(\text{NH}_3)_4(\text{H}_2\text{O})\text{RhOOH}^{2+}$ at or near its 241-nm absorption maximum. The sulfides CH_3SPh and $(2\text{-C}_3\text{H}_7)_2\text{S}$ have poor solubility in water, and their reactions were studied in water-acetonitrile solvent mixtures. The ionic strength was maintained with NaClO_4 , mostly at 0.10 M, but was raised to 0.20 M for less reactive substrates to permit the use of higher acid concentrations. Sulfide concentrations were typically varied in the range 1.0–6.0 mM. Only CH_3SPh was studied at a single concentration, 1.0 mM, because the background absorbance was too large at higher concentrations, and the reactions were too slow at lower concentrations. The formation of $(\text{en})_2\text{Co}(\text{S}(\text{O})\text{CH}_2\text{-CH}_2\text{NH}_2)^{2+}$ was monitored at 365 nm. The oxidation of PPh_3 and derivatives was monitored at or close to their absorption maxima around 275–280 nm. In the $(\text{NH}_3)_4(\text{H}_2\text{O})\text{RhOOH}^{2+}$ /nitrite experiments, the nitrite solution was injected last to avoid the slow acid-induced decomposition of nitrite prior to the onset of the reaction with the hydroperoxide.^{9,11}

Isotopically labeled $(\text{NH}_3)_4(\text{H}_2\text{O})\text{RhOOH}^{2+}$ was prepared in the following way. Acetonitrile (10 mL) was vacuum-degassed in three freeze-pump-thaw cycles and saturated with $^{18}\text{O}_2$ at 5 °C. To 2 mL of this solution was added 2 mL of air-free 0.6 mM aqueous $(\text{NH}_3)_4(\text{H}_2\text{O})\text{RhH}^{2+}$ (pH ~3), and the alkalinity was adjusted with sodium hydroxide to pH 11. After 4 min, this solution of $(\text{NH}_3)_4(\text{H}_2\text{O})\text{Rh}^{18}\text{O}^{18}\text{OH}^{2+}$ was reacidified to pH 1 with perchloric acid, and 25 μL of triphenylphosphine (52 mM in AN) was injected. After about 1 h, a mass spectrum was obtained with a Finnigan TSQ700 mass spectrometer.

Results

Oxidation Products. Methyl phenyl sulfide was oxidized to the sulfoxide, eq 2, as determined by comparison of its UV-vis spectrum, Figure S1, with that of an authentic sample. The 1:1 stoichiometry in eq 2 was confirmed by spectrophotometric titration, Figure S2.



Other sulfides were assumed also to be oxidized to the corresponding sulfoxides. The thiol $\text{CH}_3\text{CH}_2\text{SH}$ was oxidized to the disulfide, $\text{CH}_3\text{CH}_2\text{SSCH}_2\text{CH}_3$, which was identified by the maximum at 245 nm ($\epsilon = 411 \text{ M}^{-1} \text{ cm}^{-1}$) in a difference UV spectrum after completion of the reaction

Table 1. Summary of Rate Constants for the Reactions of $(\text{NH}_3)_4(\text{H}_2\text{O})\text{RhOOH}^{2+}$ with Various Nucleophiles at 25 °C

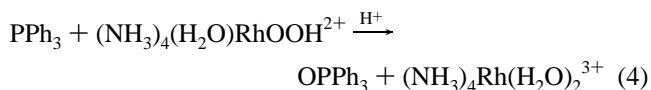
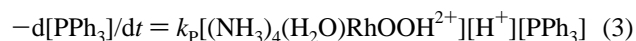
nucleophile	$k/\text{M}^{-2} \text{ s}^{-1}$	solvent (μM)
I^-	$(8.80 \pm 0.06) \times 10^3$ ^a	water (0.10)
Br^-	2.35 ± 0.05 ^a	water (0.10)
NO_2^-	$(1.54 \pm 0.10) \times 10^4$	water (0.10)
HNO_2	$(8.91 \pm 0.50) \times 10^2$	water (0.10)
$\text{P}(\text{C}_6\text{H}_5)_3$	$(3.74 \pm 0.05) \times 10^3$	50% AN (0.10)
$\text{P}(p\text{-C}_6\text{H}_4\text{-CH}_3)$	$(4.69 \pm 0.08) \times 10^3$	50% AN (0.10)
$\text{P}(p\text{-C}_6\text{H}_4\text{-F})$	$(1.89 \pm 0.03) \times 10^3$	50% AN (0.10)
$\text{P}(p\text{-C}_6\text{H}_4\text{-Cl})$	$(1.42 \pm 0.03) \times 10^3$	50% AN (0.10)
$\text{P}(p\text{-C}_6\text{H}_4\text{-CF}_3)$	$(3.72 \pm 0.04) \times 10^2$	50% AN (0.10)
$(\text{en})_2\text{Co}(\text{SCH}_2\text{CH}_2\text{NH}_2)^{2+}$	$(7.11 \pm 0.08) \times 10^2$	water (0.20)
	$(4.30 \pm 0.09) \times 10^2$	water (0.10)
	$(1.82 \pm 0.02) \times 10^2$	50% AN (0.10)
	$(1.82 \pm 0.01) \times 10^2$	water (0.20)
CH_3SPh	$(1.30 \pm 0.02) \times 10^2$	10% AN (0.20)
$(2\text{-C}_3\text{H}_7)_2\text{S}$	45.0 ± 1.0	50% AN (0.20)
$\text{C}_2\text{H}_5\text{SH}$	8.0 ± 0.4	water (0.20)
	5.0 ± 0.10	50% AN (0.20)

^a Reference 4.

between 0.40 mM $(\text{NH}_3)_4(\text{H}_2\text{O})\text{RhOOH}^{2+}$ and 6.0 mM $\text{CH}_3\text{CH}_2\text{SH}$ at 0.20 M H^+ . An authentic sample of the disulfide was used for spectral comparison. The reaction is believed to involve oxygen atom transfer to the thiol to generate the sulfenic acid, $\text{CH}_3\text{CH}_2\text{S}(\text{O})\text{H}$, which should react rapidly with an additional equivalent of thiol and form the disulfide.^{12,13}

Triphenylphosphine was oxidized to triphenylphosphine oxide, OPPh_3 , as confirmed by mass spectrometry. The reaction of $(\text{NH}_3)_4(\text{H}_2\text{O})\text{Rh}^{18}\text{O}^{18}\text{OH}^{2+}$ with PPh_3 yielded $^{18}\text{OPPh}_3$ (m/z 279, $z = 1+$) as the sole product, confirming oxygen atom transfer from the hydroperoxide.

Kinetics. The $(\text{NH}_3)_4(\text{H}_2\text{O})\text{RhOOH}^{2+}/\text{PPh}_3$ reaction yielded pseudo-first-order rate constants that varied linearly with $[\text{H}^+]$ and $[(\text{NH}_3)_4(\text{H}_2\text{O})\text{RhOOH}^{2+}]$, eq 3, and yielded a third-order rate constant $k_p = (3.74 \pm 0.05) \times 10^3 \text{ M}^{-2} \text{ s}^{-1}$. A spectrophotometric titration, Figure S3, confirmed the 1:1 stoichiometry of eq 4.



Several *p*-substituted triphenylphosphines, $\text{P}(p\text{-XPh})_3$, were also examined. The rate constants, listed in Table 1, are linearly correlated with the Hammett substituent constants 3σ as shown in Figure 1. The slope of the plot yields a reaction constant $\rho = -0.53$.

The sulfides, like the phosphines, followed a mixed third-order rate law, eq 5, and yielded the rate constants in Table 1.

The ionic strength effect in the range 0.020–0.085 M for the $(\text{CH}_2)_5\text{S}$ reaction was determined in aqueous solution. A plot of $\log k$ versus $\mu^{1/2}/(1 + \mu^{1/2})$, according to the

(9) Pestovsky, O.; Bakac, A. *Inorg. Chem.* **2002**, *41*, 3975–3982.
 (10) Endicott, J. F.; Wong, C.-L.; Inoue, T. *Inorg. Chem.* **1979**, *18*, 450–454.
 (11) Stedman, G. *Adv. Inorg. Chem. Radiochem.* **1979**, *22*, 113–170.

(12) Hogg, D. R. In *The Chemistry of Sulfenic Acids and Their Derivatives*; Patai, S., Ed.; John Wiley & Sons: New York, 1990; pp 361–402.
 (13) Arterburn, J. B.; Peryy, M. C.; Nelson, S. L.; Dible, B. R.; Holguin, M. S. *J. Am. Chem. Soc.* **1997**, *119*, 9309–9310.

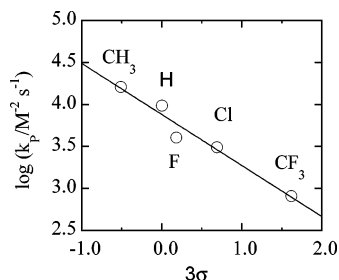
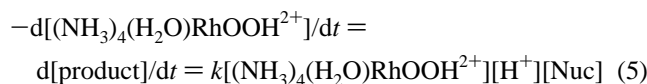


Figure 1. Plot of $\log(k_p)$ vs 3σ for the reaction of $(\text{NH}_3)_4(\text{H}_2\text{O})\text{RhOOH}^{2+}$ with *p*-substituted triphenylphosphines.

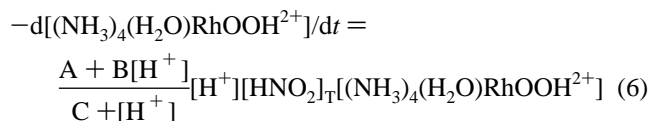


Bronsted–Debye–Hückel equation,¹⁴ is a straight line with a slope of 2.0, Figure S4. This value supports the assignment of a 2+ charge for the hydroperoxide.

The reaction of $\text{CH}_3\text{CH}_2\text{SH}$ with $(\text{NH}_3)_4(\text{H}_2\text{O})\text{RhOOH}^{2+}$ in 1:1 AN–water yielded $k = 5.0 \text{ M}^{-2} \text{ s}^{-1}$. In aqueous solutions ($\leq 3\%$ CH_3CN) at $[\text{H}^+] = 0.20 \text{ M}$, a pseudo-second-order rate constant $k = 1.6 \text{ M}^{-1} \text{ s}^{-1}$ was determined. Under the likely assumption that the rate law retains the $[\text{H}^+]$ -term, the third-order rate constant $k = 8.0 \text{ M}^{-2} \text{ s}^{-1}$ is obtained.

The oxidation of $(\text{en})_2\text{Co}(\text{SCH}_2\text{CH}_2\text{NH}_2)^{2+}$ by $(\text{NH}_3)_4(\text{H}_2\text{O})\text{RhOOH}^{2+}$ also takes place according to the rate law of eq 5. The slope of the linear plot of $k_{\text{obs}}/[\text{H}^+]$ versus $[(\text{en})_2\text{Co}(\text{SCH}_2\text{CH}_2\text{NH}_2)^{2+}]$ in Figure S5 gives $k = 711 \pm 8 \text{ M}^{-2} \text{ s}^{-1}$.

The oxidation of $\text{HNO}_2/\text{NO}_2^-$ with limiting amounts of $(\text{NH}_3)_4(\text{H}_2\text{O})\text{RhOOH}^{2+}$ in 3–100 mM aqueous HClO_4 at 0.10 M ionic strength followed pseudo-first-order kinetics. The dependence on $[\text{H}^+]$ and nitrite is described in eq 6, where $[\text{HNO}_2]_{\text{T}}$ represents the total concentration of nitrite ($[\text{NO}_2^-] + [\text{HNO}_2]$).



The fitting of all the data to the expression in eq 6 yielded $A = (19.7 \pm 3.4) \text{ M}^{-1} \text{ s}^{-1}$, $B = 853 \pm 82 \text{ M}^{-2} \text{ s}^{-1}$, and $C = (1.55 \pm 0.70) \times 10^{-3} \text{ M}$. A plot of $k_{\text{obs}}/([\text{H}^+][\text{HNO}_2]_{\text{T}})$ versus $[\text{H}^+]$ and the fit to eq 6 are shown in Figure 2. The data suggest the mechanism in Scheme 1, according to which both HNO_2 and NO_2^- , related by the protolytic equilibrium in eq 7, react with $(\text{NH}_3)_4(\text{H}_2\text{O})\text{RhOOH}^{2+}$ in acid-catalyzed reactions of eqs 8–9.

The rate law for Scheme 1, eq 10, has the same general form as eq 6, and identifies parameters A , B , and C as k_0K_a , k_1 , and K_a , respectively. The value of $C = K_a = 1.55 \times 10^{-3} \text{ M}$ agrees reasonably well with the reported acidity constant for HNO_2 , $1.15 \times 10^{-3} \text{ M}$ (25°C , $\mu = 0.50 \text{ M}$).¹⁵ When the calculations were repeated with K_a fixed at

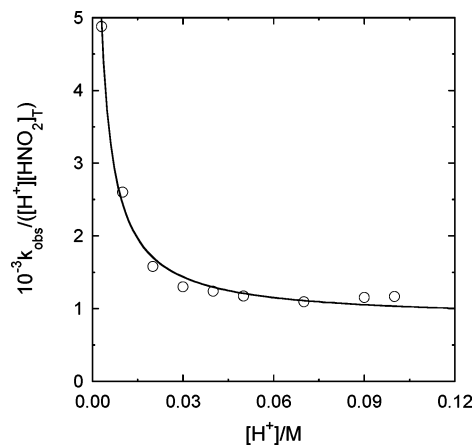
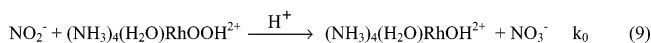
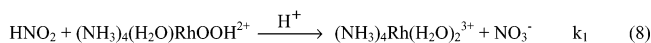
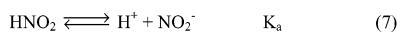


Figure 2. Plot of $k_{\text{obs}}/([\text{H}^+][\text{HNO}_2]_{\text{T}})$ vs $[\text{H}^+]$ for the reaction of $\text{HNO}_2/\text{NO}_2^-$ with $(\text{NH}_3)_4(\text{H}_2\text{O})\text{RhOOH}^{2+}$. The line is the fit to eq 6.

Scheme 1



$1.15 \times 10^{-3} \text{ M}$, the individual rate constants refined to $k_0 = A/K_a = (1.54 \pm 0.04) \times 10^4 \text{ M}^{-2} \text{ s}^{-1}$ and $k_1 = 891 \pm 50 \text{ M}^{-2} \text{ s}^{-1}$. A summary of all the kinetic data is given in Table 1.

rate =

$$\frac{k_0K_a + k_1[\text{H}^+]}{K_a + [\text{H}^+]}[\text{H}^+][\text{HNO}_2]_{\text{T}}[(\text{NH}_3)_4(\text{H}_2\text{O})\text{RhOOH}^{2+}] \quad (10)$$

Discussion

All the reactions of $(\text{NH}_3)_4(\text{H}_2\text{O})\text{RhOOH}^{2+}$ in Table 1 exhibit first-order dependence on $[\text{H}^+]$. Acid catalysis also dominates O-atom transfer from other hydroperoxometal complexes and appears to be a general feature of such reactions.^{4,5,7}

The rate constants in Table 1 cover a range of almost 4 orders of magnitude. In qualitative terms at least, the more nucleophilic the substrate, the faster the reaction. The same trend is observed within a series of triphenylphosphines, for which a reaction constant $\rho = -0.53$ was obtained. The large negative value of ρ is indicative of a nucleophilic attack by the phosphines at one of the oxygens of the protonated hydroperoxide.

Pentamethylene sulfide, $(\text{CH}_2)_5\text{S}$, is about twice as reactive as 1,4-dithiane ($(\text{CH}_2)_4\text{S}_2$), consistent with the greater nucleophilicity of the former. The effect runs contrary to the statistical considerations, which would predict dithiane, with two sulfur sites, to react faster.

The change of solvent from water to 1:1 AN–water caused the rate constants for the reactions of $(\text{CH}_2)_5\text{S}$ and $\text{C}_2\text{H}_5\text{SH}$ to decrease (Table 1). It is not clear whether the effect arises from the changes in the acidity of protonated hydroperoxide or its reactivity in oxygen transfer.

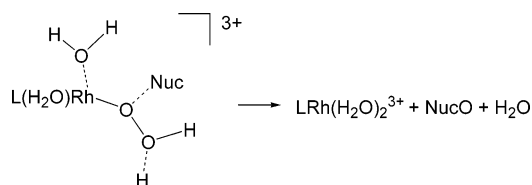
The most intriguing mechanistic issue in all of the reactions in Table 1 is the site of proton attack. It is generally

(14) Espenson, J. H. *Chemical Kinetics and Reaction Mechanisms*, 2nd ed.; McGraw-Hill: New York, 1995.

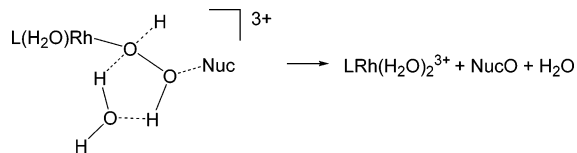
(15) Smith, R. M.; Martell, A. E. *Critical Stability Constants*; Plenum: New York, 1976; Vol. 4.

Hydroperoxorhodium

Scheme 2



Scheme 3



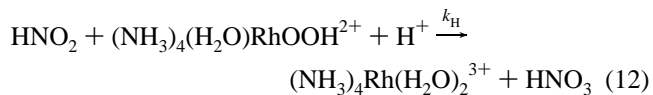
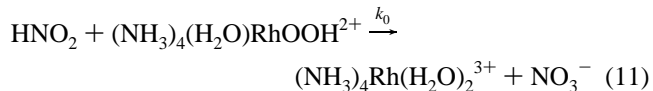
believed that protonation at the metal-bound oxygen leads to the dissociation of H_2O_2 , although this may not be the case for substitutionally inert metals such as Rh(III). If the productive chemistry does utilize the hydroperoxide protonated at the remote oxygen, and the nucleophile attacks at the less electrophilic adjacent oxygen, then the picture is completed by the departure of H_2O and entry of a molecule of solvent to complete the coordination sphere around the metal, Scheme 2.

Another possibility is shown in Scheme 3, where the more electron-rich adjacent oxygen is protonated, and the attack by nucleophile takes place at the more accessible remote site. In this scenario, a hydrogen-bonded molecule of water facilitates proton shift between the two oxygens in concert with O-transfer to the nucleophile. The two mechanisms might be distinguished by proper isotope labeling, but such experiments have not been carried out yet.

The acid dependence for the reaction between $(\text{NH}_3)_4(\text{H}_2\text{O})\text{RhOOH}^{2+}$ and $\text{HNO}_2/\text{NO}_2^-$, eq 6, was explained by

Scheme 1. In this proposal, HNO_2 and NO_2^- both react with the hydroperoxide in parallel acid-catalyzed reactions, pictured as nucleophilic substitutions at a peroxo oxygen, Scheme 2 or 3, similar to that proposed earlier for the reactions of several peroxides with nitrite anions.¹⁶

The data alone cannot, however, rule out an alternative mechanism having only one form, HNO_2 , react by an acid-independent and an acid-catalyzed path, eqs 11 and 12.



We consider this interpretation less likely not only because this would be the only example in our work where both pathways operate, but especially because the acid-independent term would dominate, opposite to the reactions of all the other nucleophiles in Table 1. Moreover, it is difficult to see how the less nucleophilic HNO_2 could be the sole reactive form, and the stronger nucleophile, NO_2^- , unreactive.

Acknowledgment. We are thankful to Dr. Oleg Pestovsky for his experimental assistance. This manuscript has been authored by Iowa State University under Contract W-7405-ENG-82 with the U.S. Department of Energy.

Supporting Information Available: Nine figures and six tables with spectral, stoichiometric, and kinetic data. This material is available free of charge via the Internet at <http://pubs.acs.org>.

IC049421Y

(16) Edwards, J. O.; Mueller, J. J. *Inorg. Chem.* **1962**, *1*, 696–699.